Membrane-associated guanylate kinase-like properties of β-subunits required for modulation of voltage-dependent Ca^{2+} channels

Shoji X. Takahashi, Jayalakshmi Miriyala, and Henry M. Colecraft†

Calcium Signals Laboratory, Department of Biomedical Engineering, Johns Hopkins University School of Medicine, 726 Traylor Building, 720 Rutland Avenue, Baltimore, MD 21205

Edited by William A. Catterall, University of Washington School of Medicine, Seattle, WA, and approved March 8, 2004 (received for review October 15, 2003)

High-voltage-activated Ca^{2+} channels regulate diverse functions ranging from muscle contraction to synaptic transmission. Association between auxiliary β- and distinct pore-forming α_1-subunits is obligatory for forming functional high-voltage-activated Ca^{2+} channels, yet the structural determinants underlying this interaction remain poorly understood. Recently, homology modeling of Ca^{2+}-channel β_{1b}-subunit identified *src* homology 3 (SH3) and guanylate kinase (GK) motifs in a tandem arrangement reminiscent of the membrane-associated guanylate kinase (MAGUK) class of scaffolding proteins. However, direct evidence for MAGUK-like properties and their functional implications in β-subunits is lacking. Here, we show a functional requirement for both SH3 and GK domains in β_{2a}. Point mutations in either the putative β_{2a} SH3 or GK domains severely blunted modulation of recombinant L-type channels, showing the importance of both motifs for a functional α_1–β interaction. Coexpression of these functionally deficient β_{2a}-SH3 and GK mutants rescued WT currents, demonstrating trans complementation similar to that observed in MAGUKs. Truncated "hemi-β_{2a}" subunits, containing either the SH3 or GK domain, were ineffective on their own, but reconstituted WT currents when coexpressed. Moreover, the SH3 and GK domains were found to interact *in vitro*. These findings reveal MAGUK-like properties in β-subunits that are critical for α_1-subunit modulation, revise current models of α_1–β association, and predict new physiological dimensions of β-subunit function.

High-voltage-activated (HVA) Ca^{2+} channels are ubiquitous in excitable cells, where they transduce electrical signals into Ca^{2+} fluxes that drive diverse biological processes such as muscle contraction, synaptic transmission, hormone secretion, and gene expression (1–3). Structurally, HVA Ca^{2+} channels are heteromultimeric proteins composed of pore-forming α_1-subunits combined with auxiliary β-, $\alpha_2\delta$-, and sometimes γ-subunits. Seven genes encoding α_1-subunits ($Ca_V1.1$–1.4, $Ca_V2.1$–2.3), four encoding β-subunits (β_1–β_4), and three encoding $\alpha_2\delta$-subunits ($\alpha_2\delta$-1–$\alpha_2\delta$-3) have been identified (3).

Among the auxiliary proteins, β-subunits play a crucial role in the formation and behavior of all functional HVA Ca^{2+} channels. Association with βs is required for efficient membrane trafficking of α_1 (4–6), increasing channel open probability (P_o) (7), and normalizing the voltage dependence of channel activation (8, 9). The physiological importance of β-subunits is demonstrated by the severe phenotypes of knockout mice: β_1 knockout is lethal at birth because of asphyxiation (10); β_{2a} knockout is embryonic lethal due to cardiac defects (11); and β_4 knockout causes the *lethargic* epileptic phenotype (12). Therefore, in-depth understanding of how βs modulate α_1 is critical for insights into the operation of HVA Ca^{2+} channels in both normal and disease states.

Primary sequence alignments indicate a modular domain structure for Ca^{2+}-channel β-subunits (see Fig. 2*A*): three variable regions susceptible to alternative splicing (domains D1, D3, and D5) are separated by two highly conserved domains (D2 and D4) (13–15). This design suggests a dichotomous interpretation of β structure–function: conserved D2 and D4 participate in functions common to all βs (i.e., increasing whole-cell current amplitude, trafficking α_1-subunits to the membrane, and producing hyperpolarizing shifts in voltage dependence of activation), whereas variable domains (D1, D3, and D5) mediate unique functions (e.g., imparting distinct channel inactivation kinetics). Presently, it is well established that D4 plays an important role in functional properties *common* to all βs. Indeed, the paradigm for the molecular basis of the α_1–β interaction is that a conserved 30-aa region in β-subunit D4 [termed β-interaction domain (BID)] binds to a conserved 18-aa region in α_1-subunits [α-interaction domain (AID)] (14, 16, 17). Secondary interaction sites among distinct subsets of β- and α_1-subunits have been found (17–21). However, these are typically of lower affinity than the AID–BID interaction, involve the β-subunit variable domains, and produce subtle effects on channel gating properties in a β- and α_1-subtype-specific manner (17–19).

Several lines of evidence suggest that an interaction between α_1- and β-subunit D4 domains is not sufficient to reconstitute the common functional properties encoded in full-length βs. First, coexpression of α_1-subunits with β-subunit D4 does not fully recover whole-cell current amplitudes observed with full-length proteins (14). Second, *in vitro* binding of D4 to the AID is markedly reduced compared with full-length β, and no binding can be detected with further deletions (14). Third, recent biochemistry experiments show that point mutations in D2 disrupt β binding to α_1 (22), a finding inconsistent with the perceived functional independence of the D2 and D4 domains. These observations reveal serious deficits in our understanding of the β-subunit determinants underlying modulation of α_1-subunits. In particular, an important role for the D2 domain is hinted at, but what this role might be and its interrelationship with D4 is obscure.

Recently, homology modeling of β_{1b} suggested the presence of a *src* homology 3 (SH3) and guanylate kinase (GK) motif in the conserved D2 and D4 domains, respectively (23). The tandem arrangement of these motifs is characteristic of membrane-associated GK (MAGUK) proteins, which function as scaffolds to organize intracellular signaling pathways (24, 25). MAGUKs contain multiple protein interaction motifs, including one or more postsynaptic density-95 (PSD-95)/Dlg/ZO-1 (PDZ) domains, an SH3, and a GK domain that mediate their scaffolding role. Here, we explored the predicted homology between βs and MAGUKs and found a functional requirement for β-subunit SH3 and GK domains to reconstitute β modulation of α_1-subunits. The results provide a different molecular viewpoint of β-subunit structural determinants underlying functional α_1–β interactions and substantiate the linkage between βs and MAGUKs.

This paper was submitted directly (Track II) to the PNAS office.

Abbreviations: AID, α_1-interaction domain; BID, β-interaction domain; GK, guanylate kinase; HVA, high-voltage activated; MAGUK, membrane-associated GK; SH3, *src* homology 3; PSD-95, postsynaptic density-95.

†To whom correspondence should be addressed. E-mail: hcolecra@bme.jhu.edu.

Materials and Methods

DNA Cloning. For α_{1C}-GFP, the coding sequence of enhanced GFP (Clontech) was amplified and fused in-frame to the carboxyl terminus of rabbit α_{1C}/pGW1 (26) by overlap-extension PCR. WT and mutant β_{2a} constructs were generated by PCR using rat β_{2a}/pGW1 (9) as template and subcloned into pcDNA4.1 (Invitrogen) by using *Bam*HI and *Eco*RI sites. PCR constructs were verified by sequencing.

Cell Culture and Transfection. Low-passage-number HEK (human embryonic kidney) 293 cells were transiently transfected with 8 μg of α_{1C}-GFP, 16 μg of WT or mutant β_{2a}, and 3 μg of T antigen, by calcium phosphate precipitation. For trans experiments, 8 μg each of the "hemi-β_{2a}" subunits, NSH3 and GKC (see below), or β_2[L93P] and β_2[P234R] were cotransfected with α_{1C}-GFP. We chose not to use $\alpha_2\delta$ to permit unambiguous identification of functional effects specific to WT/mutant β_{2a}-subunits.

Electrophysiology. Recordings were performed at room temperature 2–3 days after transfection by using an EPC8 patch-clamp amplifier (HEKA Electronics, Lambrecht/Pfalz, Germany) controlled by PULSE software (HEKA Electronics). Micropipettes were fashioned from 1.5-mm thin-wall glass with filament (WPI Instruments, Waltham, MA); series resistance was typically 2–4 MΩ and compensated 70%. A *G–V* protocol with 20-ms step depolarizations (-40 to $+120$ mV) was used to evoke currents from a -100-mV holding potential. Tail currents were measured at -50 mV. Currents were sampled at 25 kHz and filtered at 10 kHz. Leak and capacitive transients were subtracted by P/8 protocol. External solution: 140 mM Et_4N $MeSO_3$, 10 mM Hepes, and 5 mM $BaCl_2$ (pH 7.3). Internal solution: 135 mM $CsMeSO_3$, 5 mM $CsCl_2$, 5 mM EGTA, 1 mM $MgCl_2$, 4 mM MgATP, and 10 mM Hepes (pH 7.3).

Immunoblotting. Transfected HEK 293 cells were lysed with 2× loading solution [125 mM Tris·HCl, pH 7.4/4% SDS/20% (vol/vol) glycerol/0.016% bromophenol blue/10% (vol/vol) 2-mercaptoethanol] and boiled for 10 min before resolving by SDS/PAGE. Primary antibodies to GFP (Covance) or Xpress (Invitrogen) were detected by horseradish peroxidase-conjugated secondary antibodies and enhanced chemiluminescence.

Protein Purification. Xpress-tagged NSH3 and V5-tagged GKC constructs were obtained by subcloning NSH3 or GKC cDNA into pET100/D-TOPO or pET102/D-TOPO (Invitrogen), respectively. Recombinant protein was expressed in BL21(DE3)* *Escherichia coli* cells (Invitrogen) after induction with 0.8 mM isopropyl β-D-thiogalactoside (IPTG) in LB for 5 h at 37°C. Cells were harvested by centrifugation and resuspended in lysis buffer (50 mM Tris·HCl, pH 7.5/1 mM $CaCl_2$/5 mM $MgCl_2$/20 mM DTT containing EDTA-free protease inhibitor mixture, 0.05 mg/ml lysozyme, and 1% Triton X-100). After centrifugation, the pellet was solubilized with 0.7% sarcosine and the proteins were recovered in the supernatant fraction. NSH3 and GKC proteins were purified using ProBond (Invitrogen).

Immunoprecipitation. GKC (0.5 μg) was added to anti-V5 antibody (Invitrogen) preincubated with Protein A/G-Plus beads (Santa Cruz Biotechnology) in IP buffer (50 mM Tris·HCl, pH 8.0/2 mM EDTA/1% Nonidet P-40/1% Triton X-100) for 1 h. Beads were washed three times and then incubated for 1 h with purified Xpress-tagged NSH3 (1 μg). Beads were washed three times and assayed by immunoblotting.

Data and Statistical Analysis. Recordings were analyzed off-line by using PULSEFIT (HEKA Electronics). Student's *t* test was used to assess statistical significance (defined as $P < 0.05$) by comparison to WT β_{2a}. Statistics and linear regression were performed in Microsoft EXCEL using built-in functions. For ON-gating charge measurements, currents were leak subtracted by using smooth curves fitted to leak pulses in IGORPRO (WaveMetrics, Lake Oswego, OR) and then analyzed in PULSEFIT. Data are means ± SEM.

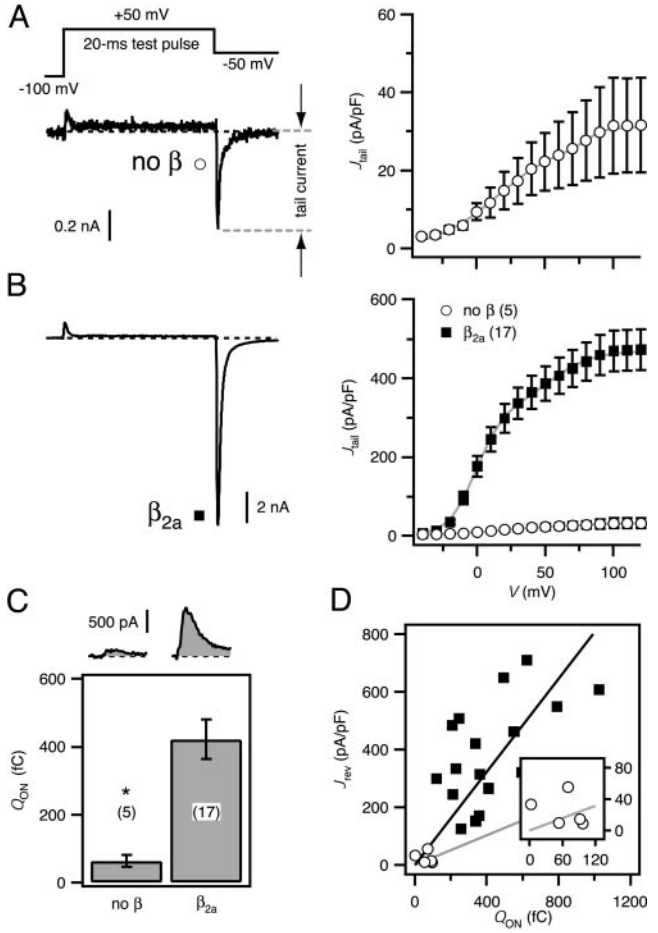

Fig. 1. Effects of β_{2a} on recombinant L-type channels reconstituted in HEK 293 cells. (*A*) (*Left*) Voltage protocol (*Upper*) and exemplar current (*Lower*) from a cell transfected with α_{1C}-GFP alone (no β). Here and throughout, exemplar currents were evoked by a 20-ms test pulse to $+50$ mV from a holding potential of -100 mV; tail currents were analyzed at -50 mV repolarization. (*Right*) Population tail-activation (*G–V*) curve for no-β channels constructed from tail-current density (J_{tail}). (*B*) Exemplar current and *G–V* curve for cotransfection of α_{1C}-GFP and β_{2a}-subunits (■). No β (○) is plotted for comparison; note difference in scale. (*C*) Exemplar ON-gating currents (*Upper*) and population ON-gating charge (Q_{ON}, *Lower*). *, $P < 0.001$; number of cells in parentheses. (*D*) Plot of tail-current density at the reversal potential (J_{rev}) vs. Q_{ON} for channels with β_{2a} (■) or no β (○). Lines are determined from linear regression of β_{2a} (black) or no β (gray). (*Inset*) Detail for no β near the origin.

Results and Discussion

Robust Modulatory Effects of β_{2a} on Recombinant L-Type Channels. A common feature among the diverse family of HVA Ca^{2+} channels is that association between auxiliary β and distinct pore-forming α_1-subunits is required to form fully functional channels (2, 3, 17). Fig. 1 demonstrates this fact by showing the profound effect of β_{2a} on recombinant L-type currents ($Ca_V1.2$; α_{1C}) reconstituted in HEK 293 cells. A carboxyl-terminus GFP-fusion construct of α_{1C} (α_{1C}-GFP) was used to permit unambiguous identification of α_{1C}-expressing cells. An ≈3-fold molar excess of β_{2a} to α_{1C}-GFP plasmid was used in transfections to ensure that fluorescent cells likely expressed both subunits. With these technical innovations, whole-cell Ba^{2+} currents were recorded from every cell chosen.

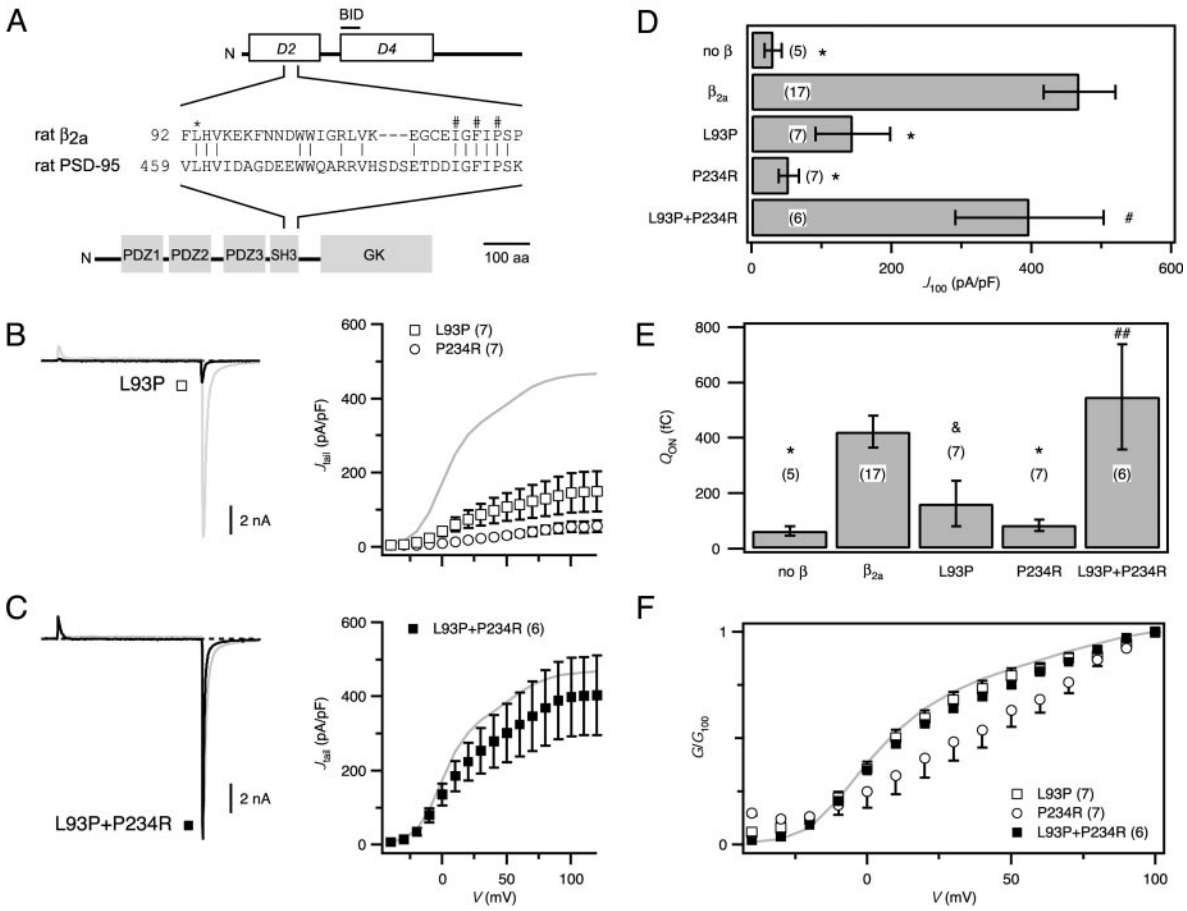

Fig. 2. Mutations in β_{2a}-SH3 and GK motifs disrupt function. (*A*) Domain structures for β_{2a} and PSD-95. The β-subunit *D4* region contains the BID, important for α_1 modulation. Sequence alignment shows homology between β_{2a} and PSD-95 in their SH3 domains. ⋆ denotes a conserved leucine residue critical for MAGUK structure–function; #s denote a trio of residues critical for α_1–β binding. (*B*) (*Left*) Exemplar current from channels reconstituted with the SH3 mutant, β_{2a}[L93P] (black). (*Right*) *G–V* curves for SH3 mutant, β_{2a}[L93P] (□) or GK mutant, β_{2a}[P234R] (○). (*C*) Functional rescue by trans complementation of SH3 and GK mutants. Exemplar current and *G–V* curve for channels reconstituted with β_{2a}[L93P] and β_{2a}[P234R] (■). (*D*) Comparison of tail-current density evoked by +100-mV test pulse (J_{100}) in channels reconstituted with different combinations of WT or mutant β_{2a}-subunits. (*E*) Q_{ON} comparison. For *D* and *E*, ⋆, $P < 0.001$, $P < 0.05$; #, $P = 0.39$; and ##, $P = 0.55$ compared with WT β_{2a}. (*F*) Comparison of normalized tail-activation curves (G/G_{100}). WT β_{2a} data (gray) are shown for reference.

Coexpression of β_{2a} with α_{1C}-GFP resulted in a dramatic increase in the amplitude of Ba^{2+} tail currents compared with those obtained with α_{1C}-GFP alone (Fig. 1 *A* and *B*). Population data indicated a nearly 15-fold enhancement of tail-current density (J_{tail}; tail-current amplitude normalized to cell capacitance) with β_{2a} (J_{tail} evoked by +100-mV step depolarization [J_{100}] was 468.9 ± 51.4 pA/pF for α_{1C}-GFP + β_{2a}; 31.5 ± 12.3 pA/pF for α_{1C}-GFP alone; $P < 0.001$). The mechanism of β_{2a} modulation of current density involved both an increase in the number of channels at the membrane (*N*) and channel open probability (P_o). Measuring the ON-gating charge (Q_{ON}) at the reversal potential (typically +50 mV) provides a convenient measure of *N* (Fig. 1*C*) (27). β_{2a} coexpression markedly increased Q_{ON} (422 ± 58 fC for β_{2a}, vs. 63 ± 17 fC for α_{1C}-GFP alone; $P < 0.001$), indicating increased surface expression of α_{1C}-GFP (Fig. 1*C*). Linear regression of J_{rev} vs. Q_{ON} provides an index of relative P_o (27). Applying this analysis indicated a larger slope, thus a higher P_o, for β_{2a}-reconstituted channels compared with those formed by α_{1C}-GFP alone (Fig. 1*D*). Overall, these results establish a robust system for investigating structure–function of α_1–β interaction and demonstrate that the use of tagged proteins does not adversely affect established parameters of β modulation of α_1-subunits in mammalian cells (5, 6, 8). This is in contrast to *Xenopus* oocytes, where β-subunit-mediated enhancement of current is reported to occur without a corresponding increase in *N*, as assessed by Q_{ON} (28).

Mutations in Either the Putative β_{2a}-SH3 or GK Motifs Disrupt Modulation. What β-subunit structural determinants mediate the impressive modulation of α_1? The prevailing model is best understood within the framework of a domain structure proposed for βs (Fig. 2*A*); three variable regions susceptible to alternative splicing (domains D1, D3, and D5) are separated by two conserved domains (D2 and D4) (13–15, 29). A previous study concluded that D4 could reconstitute the bulk of the whole-cell current amplitude when coexpressed with α_1 (14). Further refinement identified the BID (Fig. 2*A*) that interacts with a complementary AID in α_1-subunits (14). A surprising feature of this AID–BID interaction model is that it ascribes only a nominal role to the conserved D2 domain in the functions common to all βs.

Ca^{2+}-channel β-subunits are predicted to have a MAGUK-like structure from homology modeling (23). Given the rich structure–function knowledge base of MAGUKs, we explored the analogy between βs and MAGUKs to gain insights into β structure–function. We first investigated the functional importance of the putative SH3 motif in the β_{2a}-D2 domain. Partial alignment of the β_{2a}-SH3 motif with that of a prototypical MAGUK, PSD-95, revealed high sequence homology and the presence of a conserved leucine residue (L93 in β_{2a}; Fig. 2*A*) critical to MAGUK structure–function (30–33); mutation of the corresponding leucine to a proline in a *Drosophila* MAGUK, Discs large (Dlg), causes a severe

tumorigenic phenotype (34). We engineered the corresponding mutation into β_{2a} (β_{2a}[L93P]) and measured its ability to modulate L-type channels (Fig. 2*B*). β_{2a}[L93P] displayed a markedly diminished ability to reconstitute whole-cell currents as indicated by relative deficits in J_{tail} across all voltages compared to WT (Fig. 2 *B* and *D*; $J_{100} = 145 \pm 53.5$ pA/pF; $P < 0.001$). Previously, mutation of three residues in the putative β_{2a}-SH3 domain (I115/F117/P119 → AAL) was reported to completely prevent α_1-β association as assessed by coimmunoprecipitation assays (22). We found that β_{2a}[IFP→AAL] also exhibited a significantly diminished capacity to reconstitute L-type currents (not shown, $J_{100} = 166.4 \pm 66.1$ pA/pF, $n = 10$; $P < 0.001$). Overall, the marked disruptive effects of the L93P and IFP → AAL mutations on β_{2a} function revealed a surprisingly large influence of the conserved D2 domain on functional α_1–β association.

A strong piece of previous supporting evidence for the AID–BID model of α_1–β association is that a proline-to-arginine mutation in the BID (corresponding to P234R in β_{2a}) ablated β modulation of current (14). We confirmed that the mutant β_{2a}[P234R] was almost completely ineffective in supporting current (Fig. 2 *B* and *D*; $J_{100} = 53.7 \pm 14.6$ pA/pF; $P < 0.001$). Hence, independent point mutations in either D2 or D4 are both capable of severely blunting β-subunit function.

In *Drosophila* Dlg, specific mutations in either SH3 or GK motifs cause a tumorigenic phenotype (34). However, WT phenotype is obtained if SH3 and GK mutants are crossed, indicating trans complementation (34). This has also been observed between SH3 and GK mutations in PSD-95 (30, 32), and other MAGUKs (hCASK and hDlg) can dimerize (35). Therefore, we reasoned that trans complementation might similarly occur in βs, between the functionally deficient SH3 (L93P) and GK (P234R) mutants, and cause functional recovery. We tested this hypothesis by cotransfecting β_{2a}[L93P] and β_{2a}[P234R] with α_{1C}-GFP and recording whole-cell currents. Remarkably, currents were restored to virtually WT levels (Fig. 2 *C* and *D*; $J_{100} = 397.5 \pm 106.1$ pA/pF; $P = 0.21$), demonstrating trans complementation. Importantly, this result shows that both mutant proteins were expressed, ruling out the trivial explanation that loss of function of β_{2a}[L93P] and β_{2a}[P234R] was due to lack of expression. Protein expression was also directly confirmed by immunoblotting (data not shown).

Additional insights into mechanisms underlying the functionally disruptive point mutations in β_{2a}-SH3 and GK domains came from considering effects on Q_{ON} (Fig. 2*E*). Both β_{2a}[L93P] and β_{2a}[P234R] exhibited clear-cut deficits in their ability to promote increased Q_{ON}, thereby demonstrating a significantly diminished capacity to traffic α_{1C} to the membrane. By contrast, coexpression of the two complementary mutants fully recovered Q_{ON} (Fig. 2*E*). To examine possible changes in gating modulation, we compared the voltage dependence of activation among the different groups by using normalized tail-activation curves (normalized to the current evoked by +100-mV test pulse; G/G_{100}). This comparison revealed a fundamental qualitative difference between the two β_{2a} mutants. Whereas β_{2a}[L93P] produced currents that activated with a voltage dependence indistinguishable from those produced by WT β_{2a} (Fig. 2*F*), channels reconstituted with β_{2a}[P234R] activated at more depolarized potentials.

Overall, these results implicate both the SH3 and GK motifs as key players in mediating the modulatory functions of β-subunits. The results also suggest that while distinct mutations in either the SH3 or GK domain are disruptive, they are not functionally equivalent. Finally, the successes encountered in these initial experiments encouraged further exploration of the analogy between β-subunits and MAGUKs.

β-Subunit SH3 and GK Domains Present on Different Molecules Can Associate to Reconstitute a Functional Unit. To sharpen our understanding of the roles played by the SH3 and GK motifs in β-subunit function, we turned to another experimental paradigm inspired by previous work in which isolated SH3 and GK domains from PSD-95 and other MAGUKs were found to interact in yeast two-hybrid assays (30, 32, 35). We reasoned that separated β_{2a}-SH3 and GK domains might similarly interact to reconstitute a functional unit. To test this hypothesis, we designed two hemi-β_{2a} fragments loosely based on boundaries identified from the SH3–GK structure of PSD-95 (31, 33). NSH3 (residues 1–133) encompassed the SH3 domain; GKC (residues 130–604) encompassed the GK domain (see Fig. 4*A*). We first determined whether a physical interaction between β_{2a}-SH3 and GK domains could be demonstrated by using epitope-tagged NSH3 and GKC proteins expressed and purified from bacteria (Fig. 3*A*). Immobilized, V5-tagged GKC was able to pull down Xpress-tagged NSH3 (Fig. 3*B*), demonstrating a direct interaction between the two hemi-β_{2a} fragments. These data are in agreement with a recent report that two proteolytically cleaved fragments of Ca^{2+}-channel β-subunits (corresponding closely to NSH3 and GKC) directly interact *in vitro* (36).

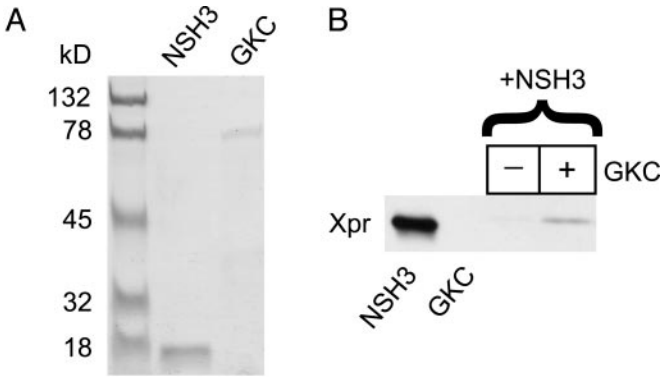

Fig. 3. β_{2a}-subunit SH3 and GK domains interact. (*A*) Coomassie blue-stained SDS/PAGE of purified Xpress-tagged NSH3 and V5-tagged GKC. (*B*) GKC pull-down of NSH3, and anti-express immunoblot (Xpr). Lane 1, purified Xpr-NSH3; lane 2, purified V5-GKC; lanes 3 and 4, pull-down of Xpress-NSH3 in the absence or presence of immobilized V5-GKC, respectively.

We next sought direct electrophysiological evidence of whether the independent hemi-β_{2a} fragments could reconstitute whole-cell currents. Expressed with α_{1C}-GFP, NSH3 was completely ineffective in rescuing current (Fig. 4 *B* and *D*; $J_{100} = 47.7 \pm 10.2$ pA/pF; $P < 0.001$), in agreement with previous findings that D2 could not function autonomously in this regard (14). GKC was only marginally more effective than NSH3 in rescuing current (Fig. 4 *B* and *D*; $J_{100} = 126.9 \pm 38.9$ pA/pF; $P < 0.001$). The rather anemic performance of GKC (which includes all of D4) in reconstituting current was unexpected, given a previous result that the D4 domain of β_{1b} could rescue the bulk of α_{1A} current (14, 17). A potential explanation for this discrepancy is the use of different experimental systems. In the *Xenopus* oocyte system used in the previous study, the presence of an endogenous β, which is variably expressed and participates in the trafficking of exogenous α_1, could seriously complicate interpretation of coexpression studies (20).

The important finding came from experiments where NSH3 and GKC were cotransfected with α_{1C}-GFP. Remarkably, in sharp contrast to the relative lack of effect of the individual fragments, NSH3 and GKC together reconstituted WT currents (Fig. 4 *C* and *D*; $J_{100} = 363.8 \pm 99.7$ pA/pF; $P = 0.38$). These results specifically demonstrated a cooperative relationship between the two unequal hemi-β_{2a} fragments in the restoration of whole-cell current amplitude. Neither NSH3 nor GKC alone could transport α_{1C} to the membrane (Fig. 4*E*);

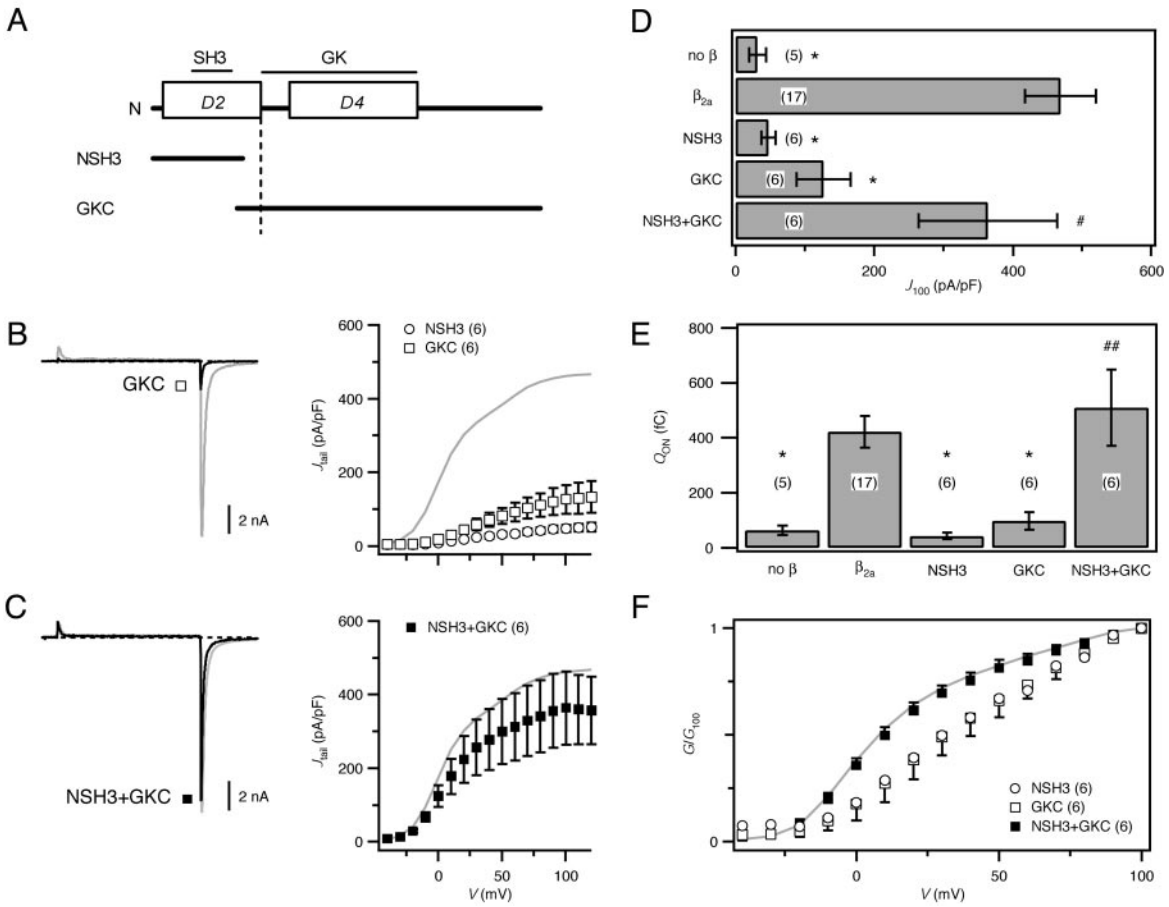

Fig. 4. β_{2a} function restored by hemi-β_{2a} fragments. (*A*) Mapping of putative SH3 and GK motifs onto β-subunit domain structure. Hemi-β_{2a} constructs included either the SH3 (NSH3) or GK domain (GKC). (*B*) (*Left*) Exemplar current from channels reconstituted with GKC (black). (*Right*) *G–V* curves for channels reconstituted with NSH3 (○) or GKC (□). (*C*) Exemplar current and *G–V* curve from channels reconstituted with NSH3 and GKC (black; ■). WT β_{2a} data (gray) are shown for reference. (*D*) Comparison of J_{100} in channels reconstituted with hemi-β_{2a} combinations. (*E*) Q_{ON} comparison. In *D* and *E*, *, $P < 0.001$; #, $P = 0.38$; and ##, $P = 0.58$ compared with WT β_{2a}; number of cells is in parentheses. (*F*) G/G_{100} comparison.

however, coexpression of NSH3 and GKC fully reconstituted the trafficking function, as indicated by Q_{ON} measurements (Fig. 4*E*). Consideration of the effects of different hemi-β_{2a} combinations on the voltage dependence of channel activation yielded important information on the requirement for both SH3 and GK domains in recapitulating β_{2a} functional effects (Fig. 4*F*). Neither NSH3 nor GKC alone produced a hyperpolarizing shift in the voltage dependence of activation, whereas coexpressing the two fragments recapitulated the leftward shift in voltage dependence of activation observed with WT β_{2a} (Fig. 4*F*).

Overall, the trans-complementation results (Fig. 2) and the hemi-β_{2a} experiments (Fig. 4) clearly demonstrated the necessity of both the SH3 and GK domains for fully restoring the common β-subunit functions of promoting increased whole-cell current amplitude, transporting α_1-subunits to the membrane, and producing hyperpolarizing shifts in the voltage dependence of channel activation. Moreover, the notion that both SH3 and GK domains are critical for functional effects, that they physically interact, and can together reconstitute a functional unit while being on separate molecules, is consistent with properties of MAGUK proteins.

Structure–Function and Physiological Implications. Our results provide clear evidence that β-SH3 and GK domains are both necessary to recapitulate full modulatory effects on pore-forming α_1 proteins. Although our experiments were conducted solely on β_{2a}, we predict that the results will apply across all βs, because the SH3 and GK motifs are present within the highly conserved D2 and D4 domains, respectively. The idea that both SH3 and GK domains are important for reconstituting functions common to all βs is a fundamental revision of prevailing models of β structural determinants underlying functional interaction with α_1-subunits (14, 17). Some of our data (lack of functional effects of β_{2a}[P234R], modest stimulatory effect of GKC on whole-cell current amplitude) are consistent with previous observations that the D4 domain is important for binding to α_1-subunits. However, our results also clearly show that binding of this domain alone to the channel is insufficient to reconstitute the bulk of functional effects on whole-cell current amplitude, channel trafficking, and activation gating.

Further work is required to elucidate how the two-pronged SH3-GK unit interacts with and tunes α_1-subunits. From the functional and biochemical data presented here, two mechanisms are possible (Fig. 5). First, an intramolecular interaction between the SH3 and GK domains could be important for β-subunit modulation of α_1 (Fig. 5*A*, one-site model). Alternatively, the β-subunit SH3 and GK domains could bind to distinct and independent sites on α_1-subunits and require no interaction between the two domains for transduction into a functional response (Fig. 5*A*, two-site model). Distinguishing between these models will require the development of β-subunit mutants that

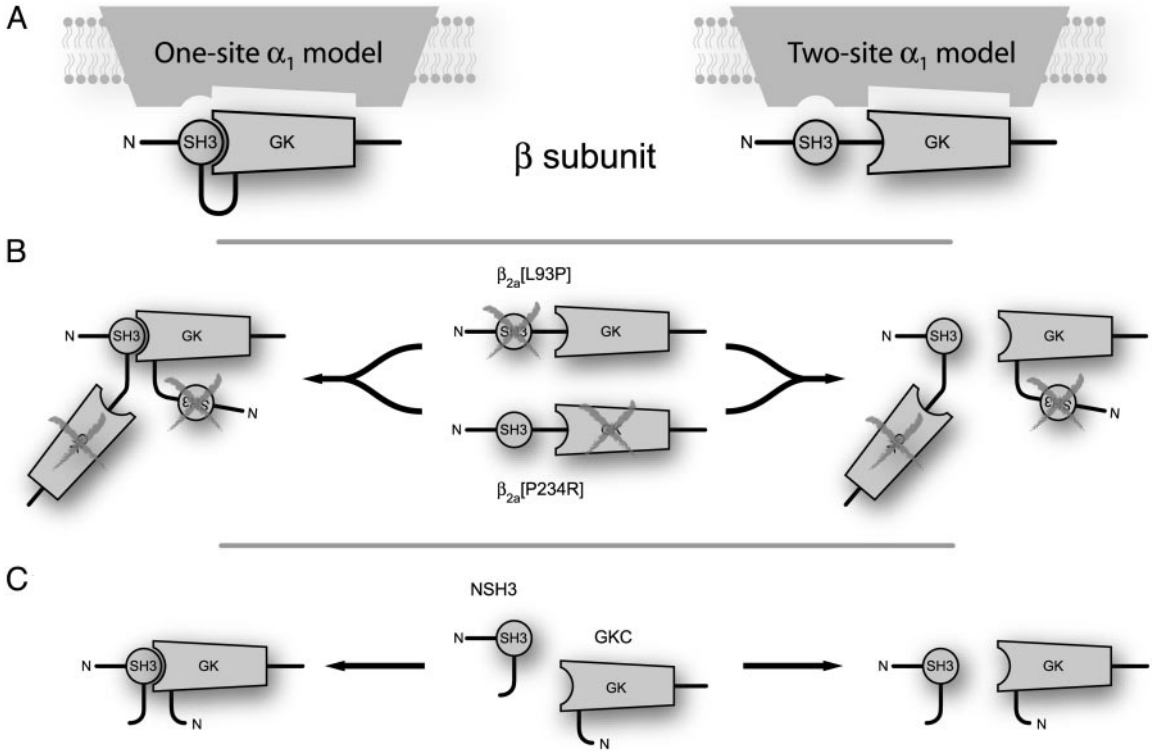

Fig. 5. Conceptualization of β-structural determinants for modulation of α_1-subunits. (*A*) In WT β, intramolecular SH3 and GK interaction could form a functional unit that modulates α_1-subunits (one-site model; *Left*). By contrast, SH3 and GK domains could interact with independent binding sites on α_1 (two-site model; *Right*). (*B*) SH3 and GK mutants are functionally deficient. However, trans complementation could reconstitute a functional unit (one-site model; *Left*) or separately provide WT SH3 and GK domains to accommodate independent binding sites (two-site model; *Right*). (*C*) Hemi-β_{2a}-subunits could operate similarly.

display no interaction between SH3 and GK domains and the identification of possible SH3-binding sites on α_1-subunits. Such work remains an important challenge for the future.

Apart from the structure–function implications, this work is distinguished by substantiating the linkage between βs and MAGUKs. Because MAGUKs serve as scaffolding proteins that organize signaling pathways, this classification has enormous ramifications for β-subunit function beyond their traditional role as auxiliary proteins to α_1. Further investigation into structure–function and potential protein interaction partners of β-subunits will likely expand the physiological roles ascribed to them.

We thank Bonnie Lonze, Amir Kashani, and Badr Alseikhan for biochemistry advice, Nick Perchiniak and Jamie Stratton for technical assistance, and David Yue for comments on the manuscript. This work was supported by grants from the National Institutes of Health (to H.M.C.) and the Medical Scientist Training Program (to S.X.T.).

1. Tsien, R. W. & Tsien, R. Y. (1990) *Annu. Rev. Cell Biol.* **6,** 715–760.
2. Hille, B. (2001) *Ion Channels of Excitable Membranes* (Sinauer, Sunderland, MA).
3. Catterall, W. A. (2000) *Annu. Rev. Cell Dev. Biol.* **16,** 521–555.
4. Chien, A. J., Zhao, X., Shirokov, R. E., Puri, T. S., Chang, C. F., Sun, D., Rios, E. & Hosey, M. M. (1995) *J. Biol. Chem.* **270,** 30036–30044.
5. Josephson, I. R. & Varadi, G. (1996) *Biophys. J.* **70,** 1285–1293.
6. Jones, L. P., Wei, S. K. & Yue, D. T. (1998) *J. Gen. Physiol.* **112,** 125–143.
7. Costantin, J., Noceti, F., Qin, N., Wei, X., Birnbaumer, L. & Stefani, E. (1998) *J. Physiol.* **507,** 93–103.
8. Singer, D., Biel, M., Lotan, I., Flockerzi, V., Hofmann, F. & Dascal, N. (1991) *Science* **253,** 1553–1557.
9. Perez-Reyes, E., Castellano, A., Kim, H. S., Bertrand, P., Baggstrom, E., Lacerda, A. E., Wei, X. Y. & Birnbaumer, L. (1992) *J. Biol. Chem.* **267,** 1792–1797.
10. Gregg, R. G., Messing, A., Strube, C., Beurg, M., Moss, R., Behan, M., Sukhareva, M., Haynes, S., Powell, J. A., Coronado, R., *et al.* (1996) *Proc. Natl. Acad. Sci. USA* **93,** 13961–13966.
11. Ball, S. L., Powers, P. A., Shin, H. S., Morgans, C. W., Peachey, N. S. & Gregg, R. G. (2002) *Invest. Ophthalmol. Visual Sci.* **43,** 1595–1603.
12. Burgess, D. L., Jones, J. M., Meisler, M. H. & Noebels, J. L. (1997) *Cell* **88,** 385–392.
13. Birnbaumer, L., Qin, N., Olcese, R., Tareilus, E., Platano, D., Costantin, J. & Stefani, E. (1998) *J. Bioenerg. Biomembr.* **30,** 357–375.
14. De Waard, M., Pragnell, M. & Campbell, K. P. (1994) *Neuron* **13,** 495–503.
15. Colecraft, H. M., Alseikhan, B., Takahashi, S. X., Chaudhuri, D., Mittman, S., Yegnasubramanian, V., Alvania, R. S., Johns, D. C., Marban, E. & Yue, D. T. (2002) *J. Physiol.* **541,** 435–452.
16. Pragnell, M., De Waard, M., Mori, Y., Tanabe, T., Snutch, T. P. & Campbell, K. P. (1994) *Nature* **368,** 67–70.
17. Walker, D. & De Waard, M. (1998) *Trends Neurosci.* **21,** 148–154.
18. Walker, D., Bichet, D., Campbell, K. P. & De Waard, M. (1998) *J. Biol. Chem.* **273,** 2361–2367.
19. Walker, D., Bichet, D., Geib, S., Mori, E., Cornet, V., Snutch, T. P., Mori, Y. & De Waard, M. (1999) *J. Biol. Chem.* **274,** 12383–12390.
20. Tareilus, E., Roux, M., Qin, N., Olcese, R., Zhou, J., Stefani, E. & Birnbaumer, L. (1997) *Proc. Natl. Acad. Sci. USA* **94,** 1703–1708.
21. Qin, N., Platano, D., Olcese, R., Stefani, E. & Birnbaumer, L. (1997) *Proc. Natl. Acad. Sci. USA* **94,** 8866–8871.
22. Gao, T., Chien, A. J. & Hosey, M. M. (1999) *J. Biol. Chem.* **274,** 2137–2144.
23. Hanlon, M. R., Berrow, N. S., Dolphin, A. C. & Wallace, B. A. (1999) *FEBS Lett.* **445,** 366–370.
24. Anderson, J. M. (1996) *Curr. Biol.* **6,** 382–384.
25. Craven, S. E. & Bredt, D. S. (1998) *Cell* **93,** 495–498.
26. Wei, X. Y., Perez-Reyes, E., Lacerda, A. E., Schuster, G., Brown, A. M. & Birnbaumer, L. (1991) *J. Biol. Chem.* **266,** 21943–21947.
27. Wei, X., Neely, A., Lacerda, A. E., Olcese, R., Stefani, E., Perez-Reyes, E. & Birnbaumer, L. (1994) *J. Biol. Chem.* **269,** 1635–1640.
28. Neely, A., Wei, X., Olcese, R., Birnbaumer, L. & Stefani, E. (1993) *Science* **262,** 575–578.
29. Takahashi, S. X., Mittman, S. & Colecraft, H. M. (2003) *Biophys. J.* **84,** 3007–3021.
30. McGee, A. W. & Bredt, D. S. (1999) *J. Biol. Chem.* **274,** 17431–17436.
31. McGee, A. W., Dakoji, S. R., Olsen, O., Bredt, D. S., Lim, W. A. & Prehoda, K. E. (2001) *Mol. Cell* **8,** 1291–1301.
32. Shin, H., Hsueh, Y.-P., Kim, E. & Sheng, M. (2000) *J. Neurosci.* **20,** 3580–3587.
33. Tavares, G. A., Panepucci, E. H. & Brunger, A. T. (2001) *Mol. Cell* **8,** 1313–1325.
34. Woods, D. F., Hough, C., Peel, D., Callaini, G. & Bryant, P. J. (1996) *J. Cell Biol.* **134,** 1469–1482.
35. Nix, S. L., Chisti, A. H., Anderson, J. M. & Walther, Z. (2000) *J. Biol. Chem.* **275,** 41192–41200.
36. Opatowsky, Y., Chomsky-Hecht, O., Kang, M. G., Campbell, K. P. & Hirsch, J. A. (2003) *J. Biol. Chem.* **278,** 52323–52332.